

Bone marrow–derived stem cells target retinal astrocytes and can promote or inhibit retinal angiogenesis

¹ATSUSHI OTANI, KAREN KINDER¹, KARLA EWALT², FRANCELLA J. OTERO², PAUL SCHIMMEL² & MARTIN FRIEDLANDER¹

Department of ¹Cell Biology, and ²Department of Molecular Biology and the Skaggs Institute for Chemical Biology, The Scripps Research Institute, La Jolla, California, USA

Correspondence should be addressed to M.F.; email: friedlan@scripps.edu

Published online: 29 July 2002, doi:10.1038/nm744

Adult bone marrow (BM) contains cells capable of differentiating along hematopoietic (Lin⁺) or non-hematopoietic (Lin⁻) lineages. Lin⁻ hematopoietic stem cells (HSCs) have recently been shown to contain a population of endothelial precursor cells (EPCs) capable of forming blood vessels. Here we show that intravitreally injected Lin⁻ BM cells selectively target retinal astrocytes, cells that serve as a template for both developmental and injury-associated retinal angiogenesis. When Lin⁻ BM cells were injected into neonatal mouse eyes, they extensively and stably incorporated into forming retinal vasculature. When EPC-enriched HSCs were injected into the eyes of neonatal *rd/rd* mice, whose vasculature ordinarily degenerates with age, they rescued and maintained a normal vasculature. In contrast, normal retinal angiogenesis was inhibited when EPCs expressing a potent angiostatic protein were injected. We have demonstrated that Lin⁻ BM cells and astrocytes specifically interact with one another during normal angiogenesis and pathological vascular degeneration in the retina. Selective targeting with Lin⁻ HSC may be a useful therapeutic approach for the treatment of many ocular diseases.

Age-related macular degeneration (ARMD) and diabetic retinopathy (DR) are the leading causes of visual loss in industrialized nations. Vision loss in these disorders results from abnormal choroidal retinal neovascularization. Because the retina consists of well-defined layers of neuronal, glial and vascular elements, relatively small disturbances, such as those seen with vascular proliferation or edema, can lead to significant loss of visual function. Inherited retinal degeneration, such as retinitis pigmentosa (RP), is also associated with vascular abnormalities such as arteriolar narrowing and vascular atrophy. Although significant progress has been made in identifying factors that promote and inhibit angiogenesis, no treatment is currently available to specifically treat ocular vascular diseases.

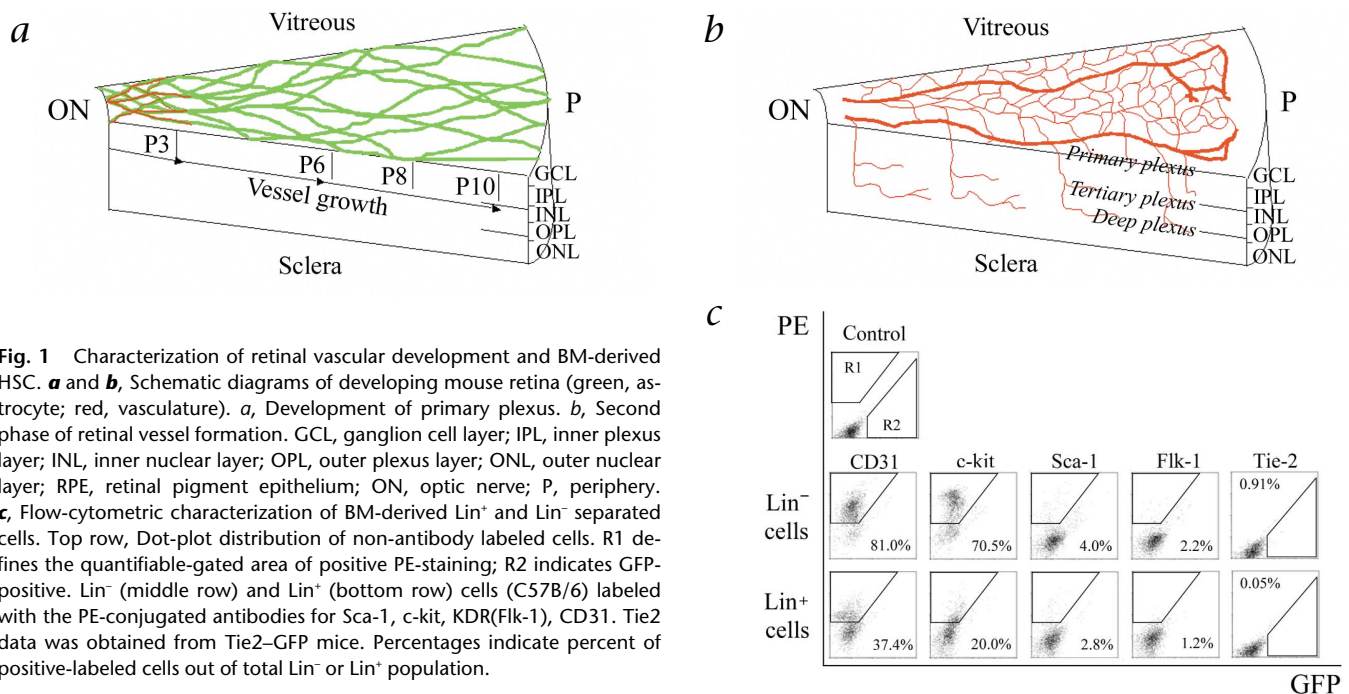
In the normal adult circulation and bone marrow (BM) there is a population of stem cells from which different sub-populations of cells can differentiate along hematopoietic (Lin⁺) or non-hematopoietic (Lin⁻) lineages. Furthermore, the Lin⁻ hematopoietic stem-cell (HSC) population contains endothelial precursor cells (EPCs) capable of forming blood vessels *in vitro* and *in vivo*¹. These cells can participate in normal and pathological postnatal angiogenesis²⁻⁴ as well as differentiate into a variety of non-endothelial cell types including hepatocytes⁵, microglia⁶, cardiomyocytes⁷ and epithelium². Although these cells have been used in several experimental models of angiogenesis, the mechanism of EPC targeting to neovasculature is unknown and there is no strategy that can effectively increase the number of cells that contribute to a particular vasculature. Here we show that intravitreal injection of Lin⁻ HSCs from BM selectively target activated retinal astrocytes. These cells also extensively incorporate into developing retinal vessels and remain stably incorporated into neovas-

culature of the mouse eye for at least two months after injection. We also show that these same cells can be used to rescue and stabilize degenerating retinal vasculature in a mouse model of retinal degeneration. Using a physiologically relevant neonatal mouse model of retinal angiogenesis, we selectively targeted neovasculature and inhibited new vessel formation without affecting pre-established vessels using a cell-based gene therapy. Because most diseases that cause vision loss involve abnormal angiogenesis, Lin⁻ HSCs or EPCs may prove useful for modulating abnormal blood-vessel growth in ARMD, DR and certain retinal degenerations associated with abnormal vasculature.

An astrocytic template guides retinal angiogenesis

During development of the murine retinal vasculature, ischemia-driven retinal blood vessels develop in close association with astrocytes. These glial elements migrate onto the neonatal retina from the optic disc along the ganglion cell layer and spread radially; a similar process occurs in the third-trimester human fetus. As the murine retinal vasculature develops, endothelial cells use this already established astrocytic template to determine the retinal vascular pattern (Fig. 1a and b)⁸. At birth, retinal vasculature is virtually absent. By postnatal day 14 (P14), the retina has developed complex primary (superficial) and secondary (deep) layers of retinal vessels coincident with the onset of vision. Initially, spoke-like peripapillary vessels grow radially over the pre-existing astrocytic network towards the periphery, becoming progressively interconnected by capillary plexus formation. These vessels grow as a monolayer within the nerve fiber through P10 (Fig. 1a). Between P7 and P8, collateral branches begin to sprout from this primary plexus and penetrate into the retina to the outer plexi-





form layer where they form the secondary, or deep, retinal plexus. By P21, the entire network undergoes extensive remodeling and a tertiary, or intermediate, plexus forms at the inner surface of the inner nuclear layer (Fig. 1b).

A neonatal mouse retinal angiogenesis model has been used to study the role of HSCs during ocular angiogenesis for several reasons. In this physiologically relevant model, a large astrocytic template exists prior to the appearance of endogenous blood vessels, permitting an evaluation of the role for cell–cell targeting during physiologically relevant angiogenesis. In addition, this consistent and reproducible neonatal retinal vascular process is known to be hypoxia-driven; in this respect, it has similarities to many retinal diseases in which ischemia is known to be involved.

Enrichment of EPCs from BM

Although cell-surface marker expression has been extensively evaluated on the EPC population found in preparations of HSC, markers that uniquely identify EPC are still poorly defined. To enrich for EPC, Lin⁺ cells (B lymphocytes (CD45), T lymphocytes (CD3), granulocytes (Ly-6G), monocytes (CD11) and erythrocytes (TER-119)) were depleted from BM mononuclear cells. Based on previous reports, we used Sca1 antigen to further enrich for EPCs. When we compared results obtained after intravitreal injection of identical numbers of either Lin⁻Sca1⁺ or Lin⁻ cells, no difference was detected between the two groups. In fact, when only Lin⁻Sca1⁻ cells were injected, far greater incorporation into developing blood vessels occurred (data not shown). Lin⁻ cells were enriched for EPCs based on functional assays (see below). Moreover, Lin⁺ populations functionally behaved differently from the Lin⁻ cells. We also evaluated epitopes commonly used to identify EPCs for each fraction (based on previously reported *in vitro* characterization studies¹). Although none of these markers were exclusively associated with the Lin⁻ fraction, all were increased 70–1,800% in the Lin⁻ versus Lin⁺ fraction (Fig. 1c). Accepted EPC markers like Flk1, Tie2 and Sca1 were poorly expressed and not used for further fractionation.

Lin⁻ HSCs contain EPC that target astrocytes

We investigated whether intravitreally injected HSCs could target specific cell types of the retina and participate in retinal angiogenesis. Approximately 1×10^5 Lin⁻ or Lin⁺ HSCs isolated from BM of adult green fluorescent protein (GFP)- or LacZ-transgenic mice were injected into postnatal day 2 (P2) mouse eyes. Four days after injection (P6), many Lin⁻ HSCs from GFP- or LacZ-transgenic mice were adherent to the retina and had the characteristic elongated appearance of endothelial cells (Fig. 2a). In many areas, the GFP-expressing cells were arranged in a pattern conforming to underlying astrocytes and resembled blood vessels. These fluorescent cells were observed ahead of the endogenous, developing vascular network (Fig. 2b). In contrast, only a small number of Lin⁺ HSCs (Fig. 2c) or adult mouse mesenteric endothelial cells (Fig. 2d) attached to the retinal surface. To determine whether injected HSCs could also attach to retinas with pre-established vessels, we injected Lin⁻ HSCs into adult eyes. Notably, no cells attached to the retina or incorporated into established, normal retinal blood vessels (Fig. 2e).

To determine the relationship between injected Lin⁻ HSCs and retinal astrocytes, we used a transgenic mouse expressing glial fibrillary acidic protein (GFAP) promoter-driven GFP. Retinas of the GFAP-GFP-transgenic mice injected with Lin⁻ HSCs from these enhanced GFP (eGFP) transgenic mice showed colocalization of the injected eGFP EPCs and existing astrocytes (Fig. 2f–h, arrows). Processes of eGFP⁺Lin⁻ HSCs conformed to the underlying astrocytic network (Fig. 2g). In P2 eyes of GFAP-GFP-transgenic mice, the injected, labeled cells attached to only astrocytes; in P6 mouse retinas, where the retinal periphery also does not yet have endogenous vessels, injected cells adhered to astrocytes in these unvascularized areas. Notably, injected, labeled cells were observed in deeper layers of the retina at the precise location where normal retinal vessels will subsequently develop (Fig. 2i, arrows).

To determine whether injected Lin⁻ HSCs are stably incorporated into the developing retinal vasculature, we examined retinal vessels at several later time points. As early as P9 (7 d after injection), Lin⁻ HSC incorporate into CD31⁺ structures (Fig. 2j). By P16

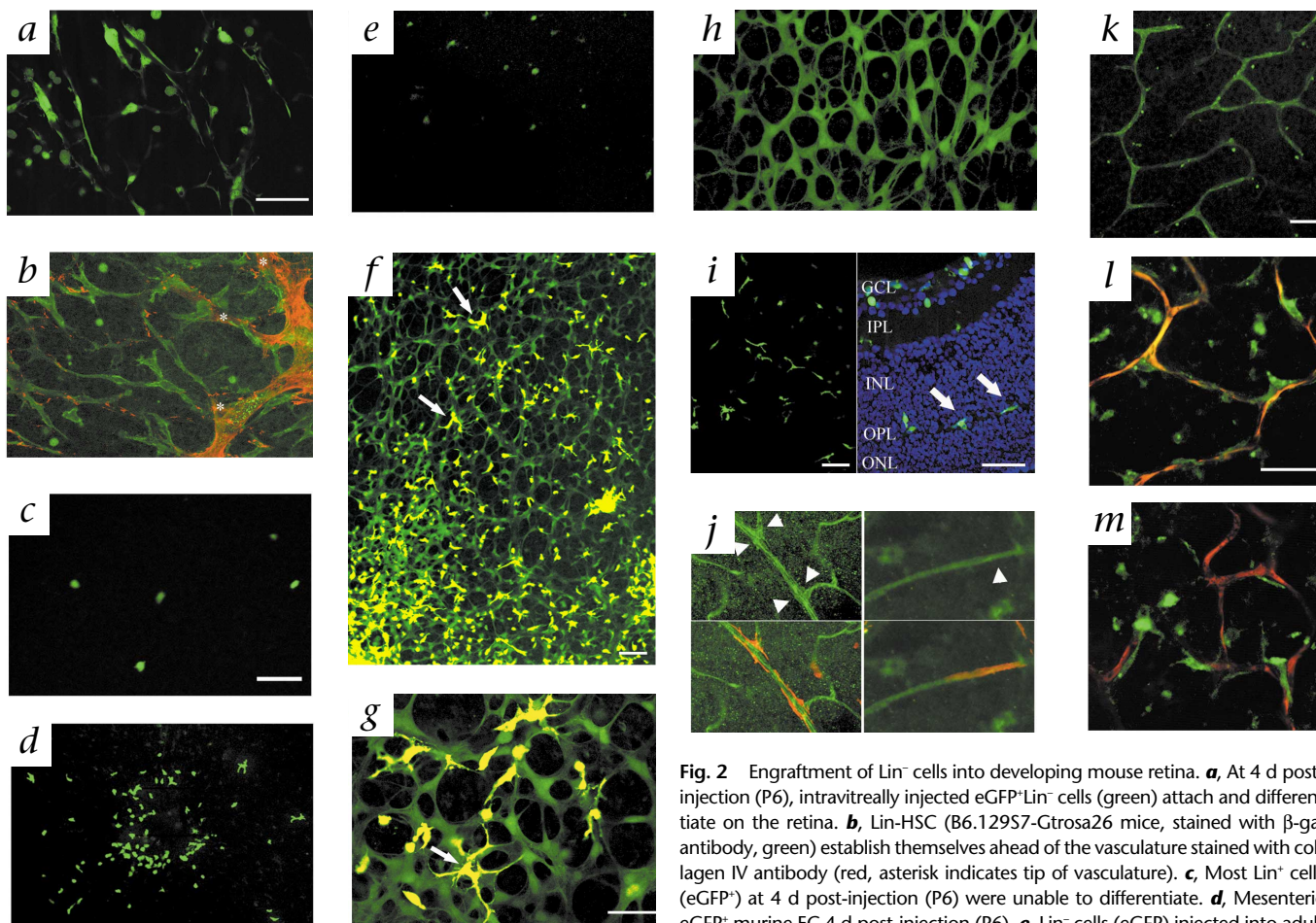


Fig. 2 Engraftment of Lin⁻ cells into developing mouse retina. **a**, At 4 d post-injection (P6), intravitrally injected eGFP⁺ Lin⁻ cells (green) attach and differentiate on the retina. **b**, Lin⁻ HSC (B6.129S7-Gtrosa26 mice, stained with β-gal antibody, green) establish themselves ahead of the vasculature stained with collagen IV antibody (red, asterisk indicates tip of vasculature). **c**, Most Lin⁺ cells (eGFP⁺) at 4 d post-injection (P6) were unable to differentiate. **d**, Mesenteric eGFP⁺ murine EC 4 d post-injection (P6). **e**, Lin⁻ cells (eGFP) injected into adult mouse eyes. **f**, Low magnification of eGFP⁺ Lin⁻ cells (yellow, arrows) homing to and differentiating along the pre-existing astrocytic template in the GFAP-GFP transgenic mouse (green). **g**, Higher magnification of association between Lin⁻ cells (eGFP) and underlying astrocyte (arrows). **h**, Non-injected GFAP-GFP transgenic control. **i**, 4 d post-injection (P6), eGFP⁺ Lin⁻ cells (green) migrate to and undergo differentiation in the area of the future deep plexus. Left panel demonstrates Lin⁻ cells (green) in a whole mounted retina; right panel is a cross section that indicates location of the Lin⁻ cells (green, arrows) in the retina. Top is vitreal side; bottom is scleral side. Blue structures are DAPI-stained nuclei. **j**, Double labeling with CD31-PE and GFP-alexa488 antibodies (colors were inverted). 7 d after injection, the injected Lin⁻ cells (GFP, red) were incorporated into the vasculature (CD31, green). Arrowheads indicate the incorporated areas. **k**, eGFP⁺ Lin⁻ cells form vessels 14 d post-injection (P17). **l** and **m**, Intracardiac injection of rhodamine-dextran (red) indicates that the vessels are intact and functional in both the primary (l) and deep plexus (m). Scale bars, 20 μm

(14 d after injection), the cells were already extensively incorporated into retinal vascular-like structures (Fig. 2k). When rhodamine-dextran was injected intravascularly (to identify functional retinal blood vessels) prior to collecting globes, most Lin⁻ HSC were aligned with patent vessels (Fig. 2l). We observed two patterns of labeled-cell distribution: first, cells were interspersed along vessels in between unlabeled endothelial cells; and in the second pattern, vessels were composed entirely of labeled cells. Injected cells were also incorporated into vessels of the deep vascular plexus (Fig. 2m). Although sporadic incorporation of HSC-derived EPC into neovasculature has been reported^{1,2}, these vascular networks are entirely composed of such cells. This demonstrates that cells from a population of BM-derived Lin⁻ HSCs injected intravitreally can efficiently incorporate into any layer of the forming retinal vascular plexus. Histological examination of non-retinal tissues (for example, brain, liver, heart, lung and BM) did not demonstrate the presence of any GFP⁺ cells when examined up to 5 or 10 days after intravitreal injection (data not shown).

These observations suggest that a sub-population of cells within the HSC Lin⁻ fraction selectively home to retinal astrocytes and stably incorporate into developing retinal vasculature. Because these cells have many characteristics of endothelial cells (association with retinal astrocytes, elongated morphology, stable incorporation into patent vessels and absence from extravascular locations), we believe these cells represent EPCs present in the Lin⁻ HSC population. The targeted astrocytes are the same cell type observed in many of the hypoxic retinopathies, and glial cells are a prominent component of neovascular fronds observed in DR and

other forms of retinal injury⁹⁻¹². Under conditions of reactive gliosis and ischemia-induced neovascularization, activated astrocytes proliferate, produce cytokines and upregulate GFAP (refs. 9,13-15), in a similar manner to neonatal retinal vascular template formation in many mammalian species, including humans¹⁶.

To test whether Lin⁻ HSCs target activated astrocytes in adult mouse eyes as they do in neonatal ones, we injected Lin⁻ HSC into adult eyes with retinas injured by photocoagulation (Fig. 3a) or needle tip (Fig. 3b). In both models, a population of cells with prominent GFAP staining occurred only around the injury site (Fig. 3a and b). Injected Lin⁻ HSCs localized to the injury site and remained specifically associated with GFAP⁺ astrocytes (Fig. 3a and b). At these sites, Lin⁻ HSCs were also observed to migrate

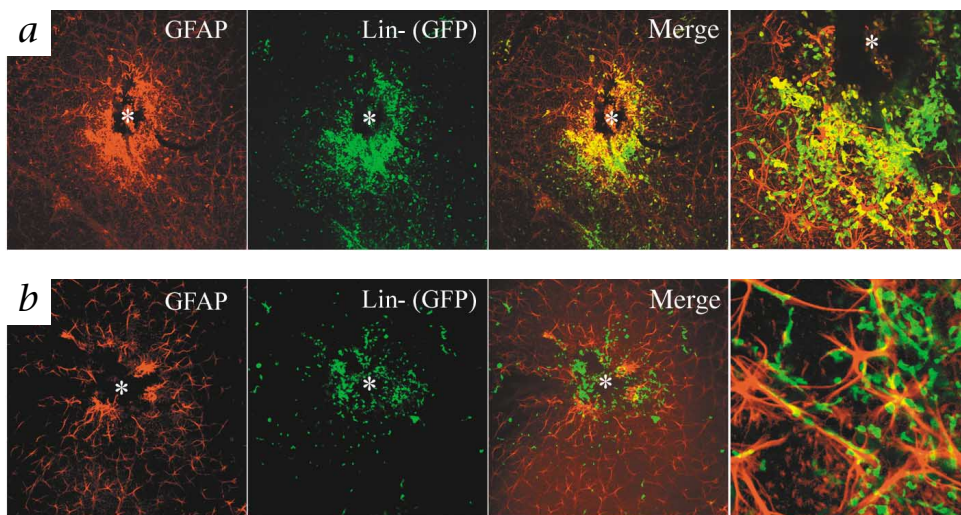


Fig. 3 Lin⁻ HSC and GFAP-expressing astrocytes localize to sites of retinal injury. **a** and **b**, eGFP⁺ Lin⁻ cells home to the gliosis (indicated by GFAP-expressing astrocytes, left, red) induced by both laser (**a**) and mechanically (**b**) induced injury in the adult retina (asterisk indicates injured site). Far right images are a higher magnification, demonstrating the close association of the Lin⁻ cells (green) and astrocytes (red).

into the deeper layer of retina at a level similar to that observed during neonatal formation of the deep retinal vasculature (data not shown). Uninjured portions of retina contained no Lin⁻ HSCs, as when Lin⁻ HSCs were injected into normal, uninjured adult retinas (Fig. 2e). These data suggest that Lin⁻ HSCs can selectively target activated glial cells in injured adult retinas with gliosis, as well as neonatal retinas undergoing vascularization.

Lin⁻ HSCs can rescue and stabilize degenerating vasculature

As intravitreally injected Lin⁻ HSC target astrocytes and incorporate into the normal retinal vasculature, these cells may stabilize degenerating vasculature in ischemic or degenerative retinal diseases associated with gliosis and vascular degeneration. To test this hypothesis, we used the *rd/rd* mouse, a model for retinal degeneration that shows marked degeneration of photoreceptor and retinal vascular layers by one month after birth. The retinal

vasculature in these mice develops normally until P16 at which time the deeper vascular plexus regresses; in most mice, the deep and intermediate plexuses are nearly completely degenerated by P30. To determine whether HSCs can rescue the regressing vessels, we injected Lin⁺ or Lin⁻ HSCs from BALB/c mice into *rd/rd* mice intravitreally at P6. By P33, after injection with Lin⁺ cells, vessels of the deepest retinal layer were nearly completely absent (Fig. 4a and b). In contrast, most Lin⁻ HSC-injected retinas have a nearly normal retinal vasculature by P33, with three parallel, well-formed vascular layers (Fig. 4c and d). Quantification of this effect showed that the average length of vessels in the deep vascular plexus of Lin⁻ injected *rd/rd* eyes was nearly three times greater than in untreated or Lin⁺ cell-treated eyes (Fig. 4e). Injection of Lin⁻ HSC from *rd/rd* adult mouse (FVB/N) BM also rescued degenerating *rd/rd* neonatal mouse retinal vasculature (Fig. 4f). Degeneration of the vasculature in *rd/rd* mouse eyes occurred as early as 2–3 weeks postnatally. Injection of Lin⁻ HSC as late as P15 also resulted in partial stabilization of the degenerating vasculature in the *rd/rd* mice for at least one month (Fig. 4g and h).

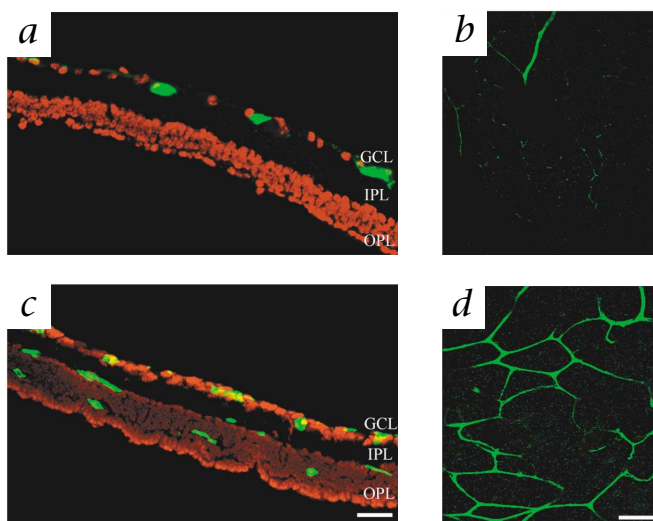
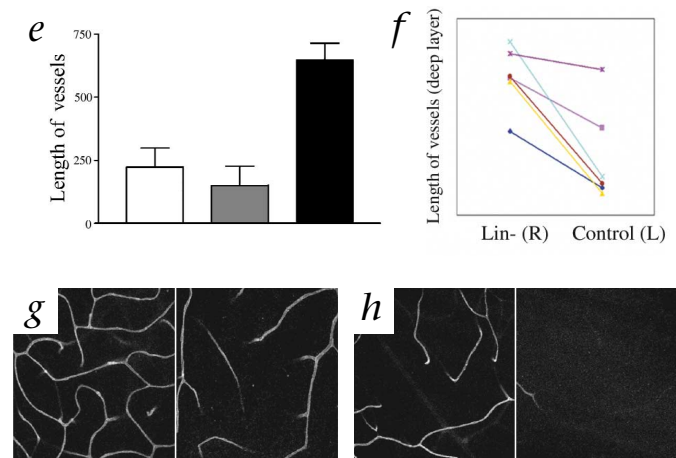


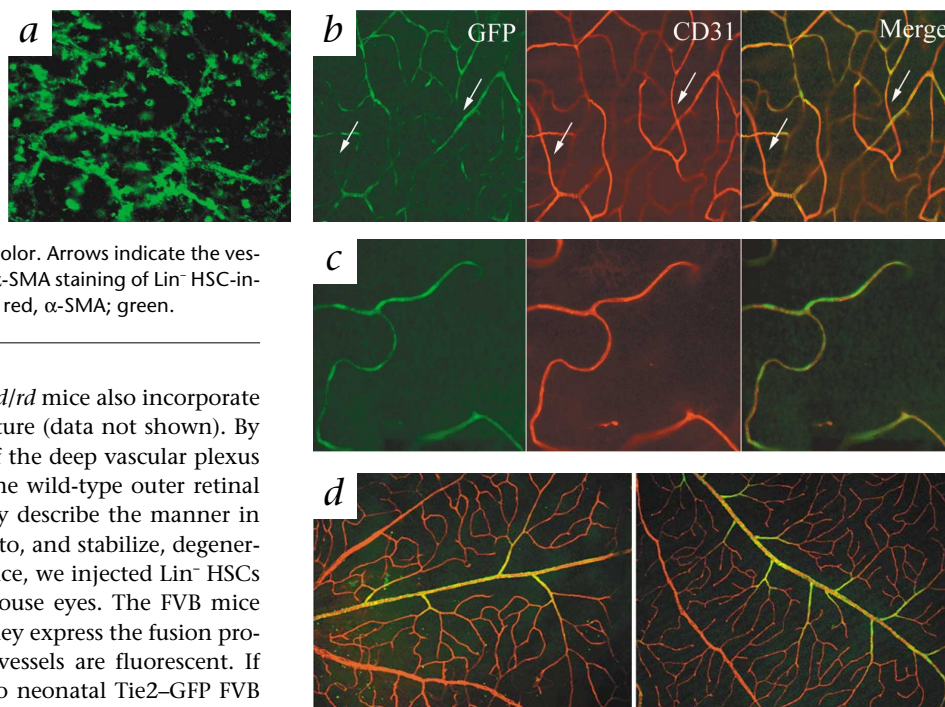
Fig. 4 Lin⁻ cells rescue the vasculature of the retinal degeneration mouse. **a–d**, Retinas at 27 d post-injection (P33) with collagen-IV staining (green). **a** and **b**, Retinas injected with Lin⁺ cells (BALB/c) showed no difference in vasculature from normal FVB mice. **c** and **d**, However, retinas injected with Lin⁻ cells (BALB/c) exhibited a rich vascular network analogous to a wild-type mouse. **a** and **c**, frozen sections of whole retina (top is vitreal side, bottom is scleral side) with DAPI staining (red). **b** and **d**, deep plexus of retinal whole mount. **e**, Bar graph illustrating the increase in vascularity of the deep vascular plexus formed in the Lin⁻ cell-injected retinas ($n = 6$). The extent of deep retinal vascularization



was quantified by calculating total length of vessels within each image. Average total length of vessels per high-power field (in microns) were compared among Lin⁻ (■), Lin⁺ (▒) or control (□) retinas. **f**, Comparison of the length of deep vascular plexus after injection with Lin⁻ (R, right eye) or Lin⁺ (L, left eye) cells from *rd/rd* mouse. The results of 6 independent mice are shown one month after injection (each color represents one mouse). **g** and **h**, Lin⁻ cells (BALB/c) also rescued the *rd/rd* vasculature when injected into P15 eyes. The intermediate (left panels) and deep (right panels) vascular plexus of Lin⁻ (**g**) or Lin⁺ (**h**) cell injected retinas (1 mo after injection) are shown. Scale bar, 20 μ m.

Fig. 5 Lin⁻ HSC integrate into, and maintain, retinal vasculature in *rd/rd* mice.

a, Deep layer of retinal whole mount (*rd/rd* mouse), 5 d post-injection (P11) with eGFP⁺Lin⁻ cells (green). **b** and **c**, P60 retinal vasculature of Tie2-GFP (*rd/rd*) mice that received BALB/c Lin⁻ cells (**b**) or Lin⁺ cell (**c**) injection at P6. The vasculature was stained with CD31 antibody (red) and only endogenous endothelial cells present green color. Arrows indicate the vessels stained with CD31 but not with GFP. **d**, α -SMA staining of Lin⁻ HSC-injected (left) and control (right) retina. CD31; red, α -SMA; green.



Lin⁻ HSC injected into younger (P2) *rd/rd* mice also incorporate into the developing superficial vasculature (data not shown). By P11, these cells migrated to the level of the deep vascular plexus and formed a pattern identical to of the wild-type outer retinal vascular layer (Fig. 5a). To more clearly describe the manner in which injected Lin⁻ HSC incorporate into, and stabilize, degenerating retinal vasculature in the *rd/rd* mice, we injected Lin⁻ HSCs of BALB/c mice into Tie2-GFP FVB mouse eyes. The FVB mice have the *rd/rd* genotype, and because they express the fusion protein Tie2-GFP, all endogenous blood vessels are fluorescent. If non-labeled Lin⁻ HSCs are injected into neonatal Tie2-GFP FVB eyes and are subsequently incorporated into the developing vasculature, there should be non-labeled gaps in the endogenous, Tie2-GFP labeled vessels that correspond to the incorporated, non-labeled Lin⁻ HSCs that were injected. Subsequent staining with another vascular marker (CD31) should delineate the entire vessel and show whether non-endogenous endothelial cells are part of the vasculature. Two months after injection, we found CD31-positive, Tie2-GFP-negative vessels in the Lin⁻ HSC-injected retinas (Fig. 5b). Most rescued vessels contained Tie2-GFP positive cells (Fig. 5c). The distribution of pericytes, as determined by staining for α -smooth-muscle actin, was not changed by Lin⁻ HSC injection regardless of whether there was vascular rescue (Fig. 5d). These data demonstrate that intravitreally injected Lin⁻ HSCs migrate into the retina, participate in the formation of normal retinal blood vessels and stabilize endogenous degenerating vasculature in a genetically defective mouse.

Inhibition of retinal angiogenesis by transfected EPCs

Because most retinal vascular diseases involve abnormal vascular proliferation rather than degeneration, we determined whether EPCs targeted to astrocytes could be used to deliver an anti-angiogenic protein and inhibit angiogenesis. We transfected Lin⁻ HSCs with T2-tryptophanyl-tRNA synthetase (T2-TrpRS). T2-TrpRS is a 43-kD fragment of TrpRS that potently inhibits retinal angiogenesis^{17,18} (Fig. 6a). On P12, retinas injected with control plasmid-transfected Lin⁻ HSCs on P2 had normal primary (Fig. 6c) and secondary (Fig. 6d) retinal vascular plexuses. When T2-TrpRS-transfected Lin⁻ HSCs were injected into P2 eyes and evaluated 10 days later, the primary network had significant abnormalities (Fig. 6e), and formation of the deep retinal vasculature was nearly completely inhibited (Fig. 6f). The few vessels observed in these eyes were markedly degenerated with large gaps between vessels. The extent of inhibition by T2-TrpRS-secreting Lin⁻ HSCs is detailed in Supplementary Table A online. T2-TrpRS is produced and secreted by Lin⁻ HSC *in vitro* (data not shown), and after injection of these cells into the vitreous, we observed a 30-kD fragment of T2-TrpRS in the retina (Fig. 6b). This 30-kD fragment was specifically observed only in retinas injected with transfected Lin⁻ HSCs, and this

decrease in apparent molecular weight compared to the recombinant or *in vitro*-synthesized protein may be due to processing or degradation of the T2-TrpRS *in vivo*. These data indicate that Lin⁻ HSCs can be used to deliver functionally active angiostatic molecules to the retinal vasculature by targeting activated astrocytes. Although it is possible that the observed angiostatic effect is due to cell-mediated activity, this seems unlikely given that eyes treated with identical but non-T2-transfected Lin⁻ HSCs showed normal retinal vasculature.

Discussion

Our finding that intravitreally injected Lin⁻ HSC localize to retinal astrocytes and incorporate into vessels suggests they may be useful in treating many retinal diseases. Although most injected HSC adhere to the astrocytic template, small numbers migrate deep into the retina, homing to regions where the deep vascular network will subsequently develop. Even though no GFAP⁺ astrocytes are observed in this area before P42 (ref. 8), this does not exclude the possibility that GFAP⁺ glial cells are already present to provide a signal for Lin⁻ HSC localization. Many diseases are associated with reactive gliosis^{11,13,19} and in DR, glial cells and their extracellular matrix are associated with pathological angiogenesis^{11-13,20,21}.

As injected Lin⁻ HSCs specifically attached to GFAP-expressing glial cells, regardless of the type of injury, it may be possible to use Lin⁻ HSCs to target pre-angiogenic lesions in the retina. For example, in the ischemic retinopathies such as diabetes, neovascularization is a response to hypoxia. By targeting Lin⁻ HSCs to sites of pathological neovascularization, it may be possible to 'stabilize' developing neovascularization, preventing abnormalities of these vessels such as hemorrhage or edema (the causes of vision loss associated with DR). This effect might, in fact, alleviate the hypoxia that originally stimulated the neovascularization. Moreover, it may be possible to effectively deliver angiostatic proteins, such as T2-TrpRS, to sites of pathological angiogenesis by using Lin⁻ HSCs and laser-induced activation of astrocytes. Because laser photocoagulation is commonly used in clinical ophthalmology, it may be possible to use this approach for many retinal diseases. Although

such cell-based approaches have been explored in cancer therapy^{2,22}, their use for eye diseases may be more advantageous as intraocular injection makes it possible to deliver large numbers of cells directly to the site of disease.

We have used markers for lineage-committed hematopoietic cells to negatively select a population of BM-derived HSCs presumed to contain EPCs. Although the sub-population of BM-derived HSCs that can serve as EPCs is not characterized by commonly used cell surface markers, the behavior of these cells in a developing or injured retinal vasculature is entirely different from that of Lin⁺ or adult endothelial-cell populations. Further subfractionation of HSC using markers such as Lin⁻Sca1⁺ did not reveal any substantial difference from the use of Lin⁻ cells alone. These cells selectively target to sites of retinal angiogenesis and participate in the formation of patent blood vessels. The absence of non-targeted Lin⁻ HSCs could be due to lack of survival by the non-EPC fraction of the total population. Whereas Lin⁻ HSC selection appears to be effective for EPCs that target and incorporate into retinal vasculature, a different selection process may be more effective in other target tissues. Further characterization of the EPC population and the molecular mechanism of its targeting to astrocytes is needed and is currently under investigation.

Inherited retinal degenerations are often accompanied by loss of retinal vasculature^{23,24}. Effective treatment of such diseases will require restoration of function as well as maintenance of complex tissue architecture. Several recent studies have explored the use of cell-based delivery of trophic factors or stem cells themselves²⁵, but some combination of both may be necessary. For example, use of growth-factor therapy to treat retinal degenerative disease resulted in unregulated overgrowth of blood vessels²⁶ re-

sulting in severe disruption of the normal retinal tissue architecture. The use of neural²⁷ or retinal²⁸ stem cells to treat retinal degenerative disease may reconstitute neuronal function, but a functional vasculature will also be necessary to maintain retinal functional integrity. We show that incorporation of Lin⁻ HSCs into the retinal vessels of *rd/rd* mice stabilized the degenerative vasculature without disrupting retinal structure. This rescue effect also occurred when the cells were injected into P15 *rd/rd* mice. Because vascular degeneration begins on P16 in *rd/rd* mice, this observation expands the therapeutic window for effective Lin⁻ HSC treatment. The vascular rescue seen in this model is substantial, but it is not clear what effect, if any, Lin⁻ HSC treatment would have on the neuroretinal degeneration typically associated with these disorders. It will be interesting to assess the effect of this treatment on visual function.

We have found that Lin⁻ HSCs contain a population of EPCs that can promote angiogenesis by targeting reactive astrocytes and incorporate into an established template without disrupting retinal structure. Thus, genetically modified autologous EPCs transplanted into ischemic or abnormally vascularized eyes may stably incorporate into new vessels and continuously deliver therapeutic molecules locally for prolonged periods of time. Such local delivery of pharmacological agents in physiologically meaningful doses may represent a new paradigm for treating currently untreatable ocular diseases.

Methods

Cell isolation and enrichment. All experiments were performed in accordance with the NIH Guide for the Care and Use of Laboratory Animals, and all experimental procedures were approved by the TSRI Animal Care and Use Committee. Bone-marrow cells were extracted from B6.129S7-Gtosa26, Tie2GFP, ACTbEGFP, FVB/NJ (*rd/rd* mice) or BALB/cBYJ adult mice (The Jackson Laboratory, Bar Harbor, Maine). Monocytes were then separated by density gradient separation using Histopaque (Sigma) and labeled with biotin conjugated lineage panel antibodies (CD45, CD3, Ly-6G, CD11, TER-119, Pharmingen, San Diego, California) for Lin⁻ selection. Lineage positive (Lin⁻) and negative (Lin⁺) cells were separated using a magnetic separation device, MACS (Miltenyi Biotech, Auburn, California). Cells were further characterized using a FACS Calibur (Beckton Dickinson, Franklin Lakes, New Jersey) using following antibodies: PE-conjugated-Sca1, c-kit, KDR and CD31 (Pharmingen, San Diego, California). For characterization of Tie2, we used Tie2-GFP BM cells.

To collect adult mouse endothelial cells, mesenteric tissue was surgically removed from ACTbEGFP mouse and placed in collagenase (Worthington, Lakewood, New Jersey) to digest followed by filtration using a 45- μ m mesh. Flow-through was collected and incubated with endothelial growth media (Clonetics, San Diego, California). Endothelial characteristics were confirmed by observing morphological cobblestone appearance, staining with CD31

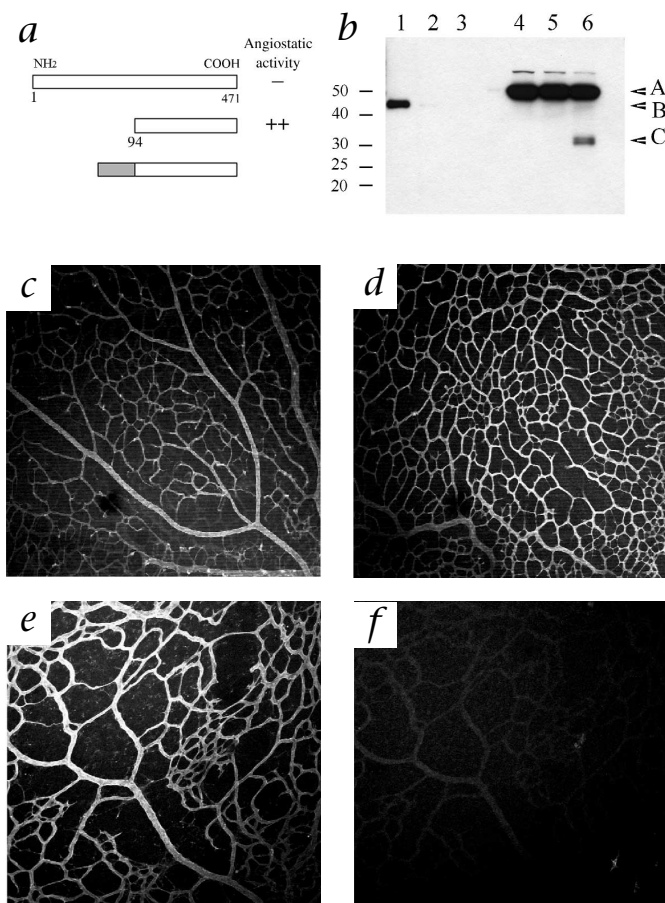


Fig. 6 T2-TrpRS-transfected Lin⁻ cells inhibit the development of mouse retinal vasculature. **a**, Schematic representation of human full-length TrpRS (top), T2-TrpRS (middle) and T2-TrpRS with an Ig- κ signal sequence at the N terminus (bottom). **b**, T2-TrpRS transfected Lin⁻ cells injected retinas express T2-TrpRS protein *in vivo*. Lanes: 1-3, varying concentrations of recombinant T2-TrpRS produced in *E. coli* (Lane 1, 2,400 pg; Lane 2, 240 pg; Lane 3, 24 pg); 4, control retina; 5, Lin⁻ cell + pSecTag2a- (vector only) injected retina; 6, Lin⁻ cell + pKLE135- (Ig- κ -T2-TrpRS in pSecTag) injected retina. A, endogenous TrpRS; B, recombinant T2-TrpRS; C, T2-TrpRS of Lin⁻ cell injected retina. **c-f**, Representative primary (superficial) and secondary (deep) plexuses of injected retinas, 7 d post-injection. **c** and **d**, Eyes injected with empty plasmid-transfected Lin⁻ cells developed normally. **e** and **f**, Most T2-TrpRS-transfected Lin⁻ cells injected eyes exhibited inhibition of deep plexus. **c** and **e**, primary (superficial) plexus; **d** and **f**, secondary (deep) plexus. Faint outline of vessels in **f** are 'bleed-through' images of primary network vessels in **e**.

monoclonal (Pharmingen) and examining cultures for the formation of tube-like structures in Matrigel (Beckton Dickinson).

Intravitreal administration of cells. An eyelid fissure was created with a fine blade to expose the P2 to P6 eyeball. Cells ($\sim 1 \times 10^5$) were then injected intravitreally using a 33-gauge needle-syringe (Hamilton, Reno, Nevada). The volume of injection was 0.5 μ l per eye.

EPC transfection. Cells were transfected using FuGENE6 Transfection Reagent (Roche, Indianapolis, IN) according to manufacturer's protocol. Lin⁻ cells (1×10^6 /ml) were suspended in opti-MEM (Gibco) containing stem-cell factor (Peprotech). DNA (1 μ g) and FuGENE (3 μ l) mixture was then added and incubated at 37 °C for 18 h. After incubation, cells were washed and collected. The transfection rate of this system was $\sim 17\%$ that was confirmed by FACS analysis. T2 production was confirmed by western-blot analysis.

Immunohistochemistry and confocal analysis. Retinas were collected at various time points and were prepared for either whole mounting or frozen sectioning. For whole mounts, retinas were fixed with 4% paraformaldehyde and blocked in 50% FBS/ 20% normal goat serum for 1 h at room temperature. Retinas were processed for primary antibodies and detected with secondary antibodies. The primaries used were: anti-Collagen IV (Chemicon, Temecula, California), anti- β -gal (Promega, Madison, Wisconsin), anti-GFAP (Dako) and anti- α -smooth muscle actin (α SMA, Dako). Secondary antibodies used were conjugated either to Alexa 488 or 594 (Molecular Probes). Images were taken using the 1024 Confocal microscope (Biorad, Hercules, California). Three-dimensional images were created using Lasersharp (Biorad) to examine the three different layers of vascular development in the whole-mount retina.

In vivo retinal angiogenesis quantification assay. For T2-TrpRS analysis, the primary and deep plexus were reconstructed from the three dimensional images. Primary plexus was divided into two categories: normal development or halted vascular progression. The categories of inhibition of deep vascular development were construed based upon the percentage of vascular inhibition including the following criteria: complete inhibition of deep plexus formation was labeled 'complete', normal vascular development (including less than 25% inhibition) was labeled 'normal' and the remainder labeled 'partial'. For the *rd/rd* mouse rescue data, 4 separate areas of the deeper plexus in each whole-mounted retina were captured using a 10 \times lens. The total length of vasculature was calculated for each image, summarized and compared among groups. To acquire accurate information, we injected Lin⁻ cells into one eye and Lin⁻ cells into another eye of the same mouse. Non-injected control retinas were taken from the same litter.

Adult retinal injury models. Laser and scar models were created using either a diode laser (150 mW, 1 s, 50 mm) or mechanically by puncturing the retina with a 27-G needle. 5 d after injury, cells were injected using the intravitreal method. Eyes were collected five days later.

Note: Supplementary information is available on the Nature Medicine website.

Acknowledgments

We thank the TSRI FACS Facility; E. Aguilar and R. Gariano for assistance with the laser-induced retinal injury model; S. Fallon, M. Ritter, M. Dorrell and G. Nemerow for helpful suggestions and J. Isner for insightful discussions. This work was supported by the National Eye Institute (EY11254 and EY12599 to M.F.), a Core Grant for Vision Research (EY 12598), the National Cancer Institute (CA92577 to P.S.), the Robert Mealey Program for the Study of Macular

Degenerations (to M.F.), and the National Foundation for Cancer Research (P.S.).

Competing interests statement

The authors declare that they have no competing financial interests.

RECEIVED 5 JUNE; ACCEPTED 2 JULY 2002

- Asahara, T. *et al.* Isolation of putative progenitor endothelial cells for angiogenesis. *Science* **275**, 964–967 (1997).
- Lyden, D. *et al.* Impaired recruitment of bone-marrow-derived endothelial and hematopoietic precursor cells blocks tumor angiogenesis and growth. *Nature Med.* **7**, 1194–1201 (2001).
- Kalka, C. *et al.* Transplantation of *ex vivo* expanded endothelial progenitor cells for therapeutic neovascularization. *Proc. Natl. Acad. Sci. USA* **97**, 3422–3427 (2000).
- Kocher, A.A. *et al.* Neovascularization of ischemic myocardium by human bone-marrow-derived angioblasts prevents cardiomyocyte apoptosis, reduces remodeling and improves cardiac function. *Nature Med.* **7**, 430–436 (2001).
- Lagasse, E. *et al.* Purified hematopoietic stem cells can differentiate into hepatocytes *in vivo*. *Nature Med.* **6**, 1229–1234 (2000).
- Priller, J. *et al.* Targeting gene-modified hematopoietic cells to the central nervous system: use of green fluorescent protein uncovers microglial engraftment. *Nature Med.* **7**, 1356–1361 (2001).
- Orlic, D. *et al.* Mobilized bone marrow cells repair the infarcted heart, improving function and survival. *Proc. Natl. Acad. Sci. USA* **98**, 10344–10349 (2001).
- Zhang, Y. & Stone, J. Role of astrocytes in the control of developing retinal vessels. *Invest. Ophthalmol. Vis. Sci.* **38**, 1653–1666 (1997).
- Dyer, M.A. & Cepko, C.L. Control of Muller glial cell proliferation and activation following retinal injury. *Nature Neurosci.* **3**, 873–880 (2000).
- MacLaren, R.E. Development and role of retinal glia in regeneration of ganglion cells following retinal injury. *Br. J. Ophthalmol.* **80**, 458–464 (1996).
- Nork, T.M., Wallow, I.H., Sramek, S.J. & Anderson, G. Muller's cell involvement in proliferative diabetic retinopathy. *Arch. Ophthalmol.* **105**, 1424–1429 (1987).
- Ohira, A. & de Juan, E. Jr Characterization of glial involvement in proliferative diabetic retinopathy. *Ophthalmologica* **201**, 187–195 (1990).
- Amin, R.H. *et al.* Vascular endothelial growth factor is present in glial cells of the retina and optic nerve of human subjects with nonproliferative diabetic retinopathy. *Invest. Ophthalmol. Vis. Sci.* **38**, 36–47 (1997).
- McLeod, D.S., D'Anna, S.A. & Lutty, G.A. Clinical and histopathologic features of canine oxygen-induced proliferative retinopathy. *Invest. Ophthalmol. Vis. Sci.* **39**, 1918–1932 (1998).
- Ridet, J.L., Malhotra, S.K., Privat, A. & Gage, F.H. Reactive astrocytes: cellular and molecular cues to biological function. *Trends Neurosci.* **20**, 570–577 (1997).
- Schnitzer, J. Astrocytes in the guinea pig, horse, and monkey retina: Their occurrence coincides with the presence of blood vessels. *Glia* **1**, 74–89 (1988).
- Wakasugi, K. *et al.* A human aminoacyl-tRNA synthetase as a regulator of angiogenesis. *Proc. Natl. Acad. Sci. USA* **99**, 173–177 (2002).
- Otani, A. *et al.* A fragment of human TrpRS as a potent antagonist of ocular angiogenesis. *Proc. Natl. Acad. Sci. USA* **99**, 178–183 (2002).
- Madigan, M.C., Penfold, P.L., Provis, J.M., BaLind, T.K. & Billson, F.A. Intermediate filament expression in human retinal macroglia. Histopathologic changes associated with age-related macular degeneration. *Retina* **14**, 65–74 (1994).
- Mizutani, M., Gerhardinger, C. & Lorenzi, M. Muller cell changes in human diabetic retinopathy. *Diabetes* **47**, 445–449 (1998).
- Rungger-Brandle, E., Dosso, A.A. & Leuenberger, P.M. Glial reactivity, an early feature of diabetic retinopathy. *Invest. Ophthalmol. Vis. Sci.* **41**, 1971–1980 (2000).
- Davidoff, A.M. *et al.* Bone marrow-derived cells contribute to tumor neovascularization and, when modified to express an angiogenesis inhibitor, can restrict tumor growth in mice. *Clin. Cancer Res.* **7**, 2870–2879 (2001).
- Wang, S., Villegas-Perez, M.P., Vidal-Sanz, M. & Lund, R.D. Progressive optic axon dystrophy and vascular changes in *rd* mice. *Invest. Ophthalmol. Vis. Sci.* **41**, 537–545 (2000).
- Matthes, M.T. & Bok, D. Blood vascular abnormalities in the degenerative mouse retina (C57BL/6-*rd* le). *Invest. Ophthalmol. Vis. Sci.* **25**, 364–369 (1984).
- Grant, M.B. *et al.* Adult hematopoietic stem cells provide functional heman-gioblast activity during retinal neovascularization. *Nature Med.* **8**, 607–612 (2002).
- Carmeliet, P. VEGF gene therapy: stimulating angiogenesis or angioma-genesis? *Nature Med.* **6**, 1102–1123 (2000).
- Ahmad, I., Tang, L. & Pham, H. Identification of neural progenitors in the adult mammalian eye. *Biochem. Biophys. Res. Commun.* **270**, 517–521 (2000).
- Tropepe, V. *et al.* Retinal stem cells in the adult mammalian eye. *Science* **287**, 2032–2036 (2000).